Biochemistry **1981**, *20*, 2133–2140

Environment of Ribothymidine in Transfer Ribonucleic Acid Studied by Means of Nuclear Overhauser Effect[†]

James Tropp and Alfred G. Redfield*

ABSTRACT: Specific nuclear Overhauser effects (NOE's) were observed from the thymine methyl proton resonance to several proton resonances in the range 6.8–11 ppm from DSS, in *Escherichia coli* tRNA$^{\mathrm{Val}}$, *E. coli* tRNA$^{\mathrm{fMet}}$, and yeast tRNA$^{\mathrm{Phe}}$. Specific reciprocal NOE's to the T methyl were also observed. The use of difference spectroscopy allowed observation of NOE's even in the aromatic region of the spectrum; all experiments were done in H_2O solvent. Cross relaxation rates for pairs of NOE-coupled resonances were determined from the NOE's to the T methyl; comparison of measured rates with theoretical rates based on tRNA$^{\mathrm{Phe}}$ crystal structure led to assignment of the fully resolved Ψ_{55} N_1 proton resonance near 10.6 ppm and the T_{54} C_6 and Ψ_{55} C_6 proton resonances near 7.3 ppm in all these tRNAs. The Ψ_{55} assignments were confirmed by NOE's between the Ψ_{55} N_1 and C_6 protons. Interatomic distances estimated from cross relaxation rates agreed with those determined by X-ray crystallography. In particular, the distance from the Ψ_{55} N_1 proton to the geometrical center of the T methyl group lay in the range 3.8–4.0 Å for all tRNAs; the range of values from four sets of tRNA$^{\mathrm{Phe}}$ X-ray coordinates was 3.4–4.1 Å. The stacking geometry of residues T_{54} and Ψ_{55} as determined by NOE resembles that found in the tRNA$^{\mathrm{Phe}}$ crystal structure. Added magnesium ion shifts the Ψ_{55} N_1 proton 0.3 ppm upfield in tRNA$^{\mathrm{Phe}}$ and 0.2 ppm in tRNA$^{\mathrm{Val}}$, but the NOE-coupled resonances shift by <0.02 ppm. Added magnesium does not affect the cross relaxation rates between the T and Ψ residues and presumably therefore does not alter their stacking geometry.

Proton NMR has been widely used to study the structure and dynamics of biological macromolecules, but published resonance assignments are frequently unreliable, and the structural inferences drawn therefrom are correspondingly vague. It is perhaps not widely appreciated that the nuclear Overhauser effect (NOE)[1] between protons can yield both unambiguous assignments and concrete structural information. For example, in favorable cases one can measure interproton distance in the range 1–4 Å with errors of <0.3 Å; the conclusions drawn in such cases are much more reliable than those derived from ring-current theory. Furthermore, the important features of NOE spectra are often interpretable by visual inspection, without recourse to elaborate computer calculations. Several investigators have studied proton NOE's of peptides and small proteins ($M_r < 10^4$) (Bothner-By, 1979; Dubs et al., 1979); work from our laboratory and a few others has shown that larger molecules such as hemoglobin, superoxide dismutase, and transfer RNA are also amenable to study (Stoesz et al., 1979; Johnston & Redfield, 1978, 1979; Bothner-By, 1979).

We report here a study of NOE's involving the thymine methyl protons of yeast tRNA$^{\mathrm{Phe}}$, *Escherichia coli* tRNA$^{\mathrm{Val}}$, and *E. coli* tRNA$^{\mathrm{fMet}}$. The T methyl resonance is well resolved in each of these tRNAs and has been convincingly assigned in previous work. We find that selective radio-frequency saturation of the T methyl peaks produces specific intensity changes (NOE's) in several proton resonances between 6.5 and 11 ppm from DSS. Analysis of these effects leads to assignment of the resolved N_1 proton resonance of residue Ψ_{55} in all three tRNAs and to a detailed picture of the base-stacking interaction between Ψ_{55} and T_{54}.

The Nuclear Overhauser Effect and Its Relation to Molecular Structure. The NOE between protons in biological macromolecules results from energy transfer between proton spins. For a given pair of protons, the rate of energy transfer is a sensitive function of the interproton distance (Noggle & Schirmer, 1971). The object of the NOE experiment is to measure the rate, from which the distance may then be calculated.

The NOE arises as follows: When radio-frequency radiation is selectively applied at the resonance frequency of a particular line in the NMR spectrum, the spins giving rise to that line absorb energy. Absorption continues until the condition of saturation is reached, at which point the irradiated line is essentially bleached from the spectrum and cannot be observed until the spins relax, i.e., give up the excess energy to their surroundings. Some portion of this energy is directly dissipated as heat in the nonspin surroundings: the rest is transferred to near neighbor spins. This tranfer results in partial saturation of the neighbor spin resonance lines; the intensities of those lines are correspondingly decreased. This decrease constitutes a nuclear Overhauser effect; for our purposes, the NOE to a resolved line is defined as the fractional intensity decrease. Overhauser *enhancements* of resonance intensity do not occur in cases of immediate interest and will not be discussed.

Consider a pair of spins labeled i and j, and suppose that spin i is irradiated. Since the relevant energy transfer processes are governed by first-order kinetics, the NOE at spin j will not appear instantaneously, but will develop gradually until a steady state is achieved. The size of the steady-state NOE will depend upon competition between the rate at which energy is transferred from spin i to spin j and the rate at which spin j can dissipate this energy to its own surroundings. These rates are referred to as the cross relaxation rate and the spin–lattice relaxation rate, respectively. A typical NOE experiment is

---

[†] From the Graduate Department of Biochemistry, Brandeis University, Waltham, Massachusetts 02254. *Received October 22, 1980.* This work was supported by U.S. Public Health Service Grant GM 20168 and by the Research Corportion. This is Publication No. 1346 of the Brandeis University Biochemistry Department. Alfred G. Redfield is also at the Physics Department and the Rosensteil Basic Medical Sciences Research Center of Brandeis University.

[1] Abbreviations used: NOE, nuclear Overhauser effect; ppm, parts per million; DSS, 3-(trimethylsilyl)-1-propanesulfonic acid sodium salt; T, ribothymidine; Ψ, pseudouridine; DEAE, diethylaminoethyl; EDTA, ethylenediaminetetraacetic acid.

0006-2960/81/0420-2133$01.25/0

based on a two-pulse sequence: saturate and observe (Redfield & Gupta, 1971). A radio-frequency pulse is applied to selectively saturate a given resonance. During the pulse, saturation is transferred to neighbor spins as described above; this causes the intensities of the neighbor spin resonance lines to decrease. Directly following the saturation pulse, the decreased intensities are monitered by the observation pulse. With the assumption that saturation of the irradiated spin is rapid compared to the relaxation rates, the time evolution of the NOE is given by (Noggle & Schirmer, 1971)

$$\mathrm{NOE} = \frac{\sigma_{ij}}{\rho_j}(1 - e^{-\rho_j t}) \qquad (1)$$

where σ_{ij} is the cross relaxation rate constant, ρ_j is the spin-lattice relaxation rate constant for spin j, and t is the duration of the saturating irradiation. Note that as $t \rightarrow \infty$ the NOE approaches the steady-state value σ_{ij}/ρ_j. Since ρ_j can be independently measured, measurements of the NOE permits determination of σ_{ij}. The theoretical maximum NOE is 1, corresponding to complete transfer of saturation.

Equation 1 describes the NOE between an isolated pair of protons. In the case of NOE's between a single proton and the three protons of a methyl group, eq 1 still applies for the effect obtained by saturating the nonmethyl proton, provided that σ_{ij} is interpreted as the cross relaxation rate between a *single* methyl proton i.e., CHD_2, and the nonmethyl proton (Tropp, 1980). For the NOE *from* the methyl group to a single nonmethyl proton, *eq 1 must be modified by replacing* σ_{ij} *with* $3\alpha_{ij}$ (Tropp, 1980).

For a pair of spins rigidly fixed in a slowly tumbling macromolecule, σ_{ij} is given (Kalk & Berendsen, 1976) by

$$\sigma_{ij} = \sigma_{ji} = \frac{-\gamma^4 \hbar^2}{10 r_{ij}^6} \tau_c \qquad (2)$$

where r_{ij} is the interproton distance and the correlation time τ_c is related to the isotropic rotational diffusion constant D by $\tau_c = (6D)^{-1}$. Other symbols have their usual meanings. Since τ_c is usually known from independent experiments, knowledge of σ_{ij} permits determination of r_{ij}. For NOE's between methyl and nonmethyl protons, eq 2 is not correct because the rapid rotation of the methyl group about its symmetry axis causes r_{ij} to fluctuate in time. It is not correct to use a weighted average of r_{ij} or r_{ij}^6; instead r_{ij} must be replaced by the square of the weighted average of r_{ij}^3 times an angle factor. The theory and some numerical results have been given elsewhere (Tropp, 1980).

Because of its sixth power dependence, σ_{ij} drops off very rapidly with increasing r. Thus, NOE's are rarely observed between spins with $r > 4$ Å. This gives the NOE experiment a selectivity which is useful in disentangling and assigning complex spectra.

However, in some cases, saturation may be serially transferred through several spins (a domino effect) leading to NOE's between protons which are physically remote. Such effects are called indirect or second-order NOE's. Second-order NOE's are usually an undesirable complication (Kalk & Berendsen, 1976), but they may often be avoided by using a sufficiently short saturation pulse (Johnson & Redfield, 1978, 1979; Tropp, 1980). On the other hand, second-order NOE's are sometimes useful (Stoesz et al., 1979).

Calculation of Theoretical Cross Relaxation Rates from Atomic Coordinates. If a crystal structure is available for the molecule being studied, theoretical values of the relevant σ_{ij} may be calculated from atomic coordinates. Proton coordinates may be grafted onto published carbon and nitrogen coordinates by using simple vector algebra and standard bond lengths and angles. The theoretical σ's then provide bench marks for interpreting experimental cross relaxation data and permit local comparisons of the crystal and solution structures.

Table I: Crystallographic Distances and Theoretical Cross Relaxation Rates for Yeast Phenylalanine tRNA[a]

	T_{54} C_6-H	Ψ_{55} N_1-H	Ψ_{55} C_6-H
T_{54} methyl	$r_c = 2.9$ Å[b] $\sigma = 2.8/s$	$r_c = 3.4$–4.1 Å[c] $\sigma = 1.8$–$0.5/s$[c]	$r_c = 5.1$ Å[d] $\sigma = 0.1/s$
T_{54} C_6-H		$r = 4.5$ Å[d] $\sigma = 0.2/s$	$r = 4.6$ Å[d] $\sigma = 0.2/s$
Ψ_{55} N_1-H			$r = 2.3$ Å[b] $\sigma = 11.4/s$

[a] For distances and rates between methyl and nonmethyl protons, r_c is the distance from the nonmethyl proton to the geometrical center of the triangle defined by the three methyl proton positions. For pairs of nonmethyl protons, r is the interproton distance. [b] Atomic coordinates taken from Voet & Rich (1971). [c] The spread of values corresponds to different sets of atomic coordinates: Sussman et al. (1978), Ladner et al. (1975), G. Quigley (personal communication), and Stout et al. (1976). [d] Calculated from orthorhombic coordinates of Ladner et al. (1975). Comparisons with other coordinates were deemed unnecessary in view of the very small predicted relaxation rates.

Table I presents the relevant σ values based on the crystal structure of yeast $tRNA^{Phe}$. Since the $tRNA^{Phe}$ structure is expected to be a good model for any class I tRNA (Sigler, 1975), the values in Table I should apply fairly well to $tRNA^{Val}$ and $tRNA^{fMet}$.

The rates between methyl and nonmethyl protons are tabulated for a *single* methyl proton, i.e., by assuming a hypothetical CHD_2 group. Details of calculations are given elsewhere (Tropp, 1980). We assumed the methyl group executes rapid rotational jumps of magnitude $2\pi/3$ radians. For the T methyl group of tRNA we chose the rotational potential minimum with one CH vector lying perpendicular to the thymine ring plane and pointing toward residue Ψ_{55}. This choice is arbitrary, but any other choice would displace the proton positions by not more than 0.2 Å, leading to small changes in the calculated σ. For example, with a methyl CH vector eclipsing the thymine 5,6 double bond, we obtain σ values ~20% larger between the methyl and T C_6 proton and ~20% smaller between the methyl and Ψ N_1 proton.

Rates between pairs of nonmethyl protons were calculated from eq 2. The rotational correlation time, τ_c, has been variously estimated to be 30 (Komoroski & Allerhand, 1972), 25 (Tao et al., 1970), and 15 ns (Schmidt et al., 1980). We chose the value 30 ns which gives good agreement between our experimental and theoretical cross relaxation rates. The smaller τ_c values would give decreases of <10% in our experimentally determined internuclear distances, which would not alter any of our subsequent conclusions.

For subsequent estimates of distances from experimental rates, the geometry used in the theory was slightly different from those used in Table I, for the case of methyl to nonmethyl NOE's. The single protons (Ψ_{55} N_1 and C_6; T_{54} C_6) were all taken to lie in a plane perpendicular to the methyl axis and passing through the methyl protons, and the stable methyl rotamer was taken to be oriented 90° with respect to that used in Table I, with one proton pointing toward Ψ_{55}. In fact, the single protons lie above or below this plane but not sufficiently so to change our conclusions.

Materials and Methods

tRNA. Yeast $tRNA^{Phe}$ was purchased from Boehringer Mannheim. Amino acid acceptance was assayed by following the standard procedure using crude yeast synthetases and was typically 1.4–1.5 nmol of phenylalanine/A_{258} unit. *E. coli* tRNAs were purified from crude tRNA (Plenum) by column chromatography of benzoylated DEAE-cellulose (Boehringer Mannheim), followed by chromatography on Sepharose 4-B and in some cases DEAE-Sephadex A-50 if required. Specific activities of the final product ranged from 1.3 to 1.6 nmol of amino acid/A_{258}, as assayed with crude *E. coli* synthetases.

NMR Samples. Except as noted, NMR samples were prepared by dialyzing small volumes of tRNA (5–6 mg in 150–190 μL) in a specially constructed flow microdialysis cell at 4 °C. For dialysis against buffers containing neither EDTA nor Mg^{2+} a small column of Chelex 100 (pretreated according to the manufacturer's instructions and then washed extensively with the appropriate buffer prior to pouring the column) was placed in series with the peristaltic pump and the dialysis cell. All buffers were prepared with glass-distilled H_2O and reagent grade chemicals by using glassware washed in 6 N HCl. Buffers for the final change of dialysis contained 5% D_2O (Wilmad, 99%, used as received) for the spectrometer field lock. Each change of dialysis was for 12 h vs. 150 mL of buffer, except for the final change where the volume was 50 mL. Samples were transferred to Wilmad microcell NMR tubes with a plastic syringe and Teflon needle.

The following buffers were used. Buffers A, B, and C contained 100 mM NaCl, 10 mM Na_2HPO_4, pH 7, 1 mM $Na_2S_2O_3$, and respectively 10, 1 and 0 mM Na_2EDTA. Buffers A′ and C′ were identical with A and C except that thiosulfate was omitted. Buffer D was similar to A but contained 5 mM $MgCl_2$; buffer D′ was identical with D except that thiosulfate was omitted.

The tRNA samples used in this study was described below. Sample 1, $tRNA^{val}$, was dialyzed against two changes of buffer A and two of buffer B. Sample 2, $tRNA^{Val}$, was dialyzed against two changes each of buffers A, and B, and C. Removal of EDTA was complete as judged by NMR. Sample 3, $tRNA^{Val}$, was dialyzed against two changes of buffer A followed by two changes of buffer D. This procedure did not remove all the EDTA; the residual impurity was estimated to be 3 mM from the NMR spectrum. After the data described herein were taken, this sample was dialyzed exhaustively against buffer D. Ten changes were required to remove the EDTA. For sample 4, $tRNA^{Phe}$, 5 mg of tRNA was dissolved in 190 μL of 100 mM NaCl, 10 mM sodium cacodylate, pH 7.0, 10 M mM EDTA, and 5% D_2O and used without dialysis. Sample 5, $tRNA^{Phe}$, was dialyzed vs. two changes of buffer A′ and two of buffer D′; removal of EDTA was complete, in contrast to sample 3 above. For sample 6, $tRNA^{fMet}$, the preparation was identical with sample 1.

NMR Data Collection. Spectra were taken on the LDB 270 spectrometer at Brandeis University; the H_2O solvent resonance was suppressed by means of the 214 observation pulse as described previously (Redfield, 1976). Nuclear Overhauser effects were recorded by using an experimental cycle based on the two-pulse saturate–observe sequence described above. In the first leg of the cycle, the saturation frequency, f_2, was set at some resonance of interest, and 16 transients of the saturate–observe sequence were collected, Fourier transformed, and accumulated. Duration of the saturation pulse was typically 200–350 ms, which sufficed to produce large first-order NOE's while avoiding extensive second-order effects (see above). The second leg of the cycle was similar to the first except that f_2 was set in some empty region of the spectrum. Thus, saturated and control (unsaturated) spectra were accumulated in parallel. At any time during a run (typically 500–1500 complete cycles) the NOE spectrum, obtained by subtracting the saturated spectrum from the control, can be displayed. We found it useful to program an extended cycle, which we refer to as the interleaved NOE experiment, in which several f_2 valves are irradiated for each control (Redfield & Kunz, 1979). In this manner we collected as many as four different NOE spectra in parallel, saving a factor of nearly 2 in running time compared to collection of a single NOE run.

Longitudinal relaxation rates, $\rho = 1/T_1$, were also measured by difference spectroscopy, using a saturation recovery method (Johnston & Redfield, 1977; Schimmel & Redfield, 1980). The experimental cycle is similar to that of the NOE experiment, except that a programmable delay time, τ, was placed between the saturation and observation pulses, and difference spectra were then recorded for several values of τ. Then, for a delay, τ, the intensity of the saturated peak in the difference spectrum is given by

$$\Delta I(\tau) = I_0 - I(\tau) \qquad (3)$$

where I_0 is the control spectrum intensity and $I(\tau)$ is the partially relaxed intensity at time τ after the end of the saturation pulse. If the recovery is exponential, a plot of ln $\Delta I(\tau)$ vs. τ yields ρ. The difference technique gives a poorer signal to noise ratio than direct saturation recovery but has the compensating advantage of providing a better base line. Care must be taken to ensure that I_0 represents the fully relaxed intensity of the peak in question; the pulse sequence duty cycle is accordingly adjusted by experimental trial.

NMR Data Reduction. Magnitudes of NOE's were determined by comparing peak heights and/or integrals of the difference spectra with those of peaks of known intensity in the control spectra. The NOE's to methyls are believed accurate to within 5% of the full methyl intensity; NOE's to other peaks are believed accurate to within 15% of a single proton intensity.

Values of σ were determined from NOE's to the methyl peaks. The measured NOE, the measured value of ρ, and the saturation time were used to solve eq 1 for σ. Equation 1 is not rigorously correct for a multispin system, but it is a good approximation in the present study where no large second-order NOE's occur. This point has been discussed in detail elsewhere (Tropp, 1980).

Results and Interpretation

Figures 1 and 2 show the low-field imino and methyl proton spectra of several tRNA samples used in this study. Figure 3 is the entire spectrum of $tRNA^{Val}$ (sample 3) downfield of H_2O; this illustrates the relative intensities of the imino (11–15 ppm from DSS) and aromatic amino and sugar regions (6–8 ppm). Figure 4 shows the NOE spectra from the T_{54} methyl resonance to the region 6–11 ppm; note that the effects are quite clean, even the region 6–8 ppm. Figure 5 is a typical action spectrum which demonstrates the specificity of the reciprocal NOE's from the aromatic amino region to the thymine methyl resonance; all NOE's from multiple proton peaks to the T methyl showed comparable specificities for all samples used in this study.

(*A*) *Samples 1 and 2, E. coli* $tRNA^{Val}$ *in 0 Magnesium.* The NOE's from these samples are virtually identical and display a pattern of interconnections, analysis of which leads to a scheme of resonance assignments which is both self-consistent and in accord with the expectation that the solution structure of any class I tRNA should resemble the crystal structure of yeast $tRNA^{Phe}$ (Sigler, 1975). Saturation of the T methyl resonance produces a large NOE at 7.42 ppm, with

Table II: Summary of NOE Data and Internuclear Distances Inferred from Them for *E. coli* Valine tRNA[a]

	obsd resonance				
irradiated resonance	0.95 ppm,[b] T_{54} methyl	6.73 ppm, G_{53} C_8 (?)	7.28 ppm, Ψ_{55} C_6-H	7.42 ppm, T_{54} C_6-H	10.78 ppm (10.57), Ψ_{55} N_1-H
0.95 ppm, T_{54} methyl		17%	<3%	50%	7%
6.73 ppm, unassigned	13% $\sigma = 0.8/s$ $r_c = 3.8$ Å		not obsd[c]	not obsd[c]	not obsd[c]
7.42 ppm, T_{54} C_6-H	38% $\sigma = 2.3/s$ $r_c = 3.1$ Å	not obsd[c]	not obsd[c]		not obsd[c]
10.78 ppm (10.57), Ψ_{55} N_1-H	11% $\sigma = 0.7/s$ $r_i = 2.9$ Å $r_c = 3.9$ Å	0%	38%	<3%	

[a] Percent NOE's (top line of each data entry) are percent intensity changes observed with 200- or 250-ms saturation. NOE's to methyl groups are given as the percent of full methyl intensity; NOE's to other protons are the percent of a single proton intensity. The distance r_c is defined in Table I; r_c values were derived from measured σ values via the model calculations described in the text. Most data are given for sample 1; results from sample 2 were virtually identical. Results for sample 3 were similar to those for samples 1 and 2 except for the resonance position of the Ψ_{55} N_1 proton, which is given in parentheses. [b] The longitudinal relaxation rate, ρ, for the T methyl resonance was 5.2 s^{-1}. [c] Possible NOE obscured by power spillover or nonspecific effects.

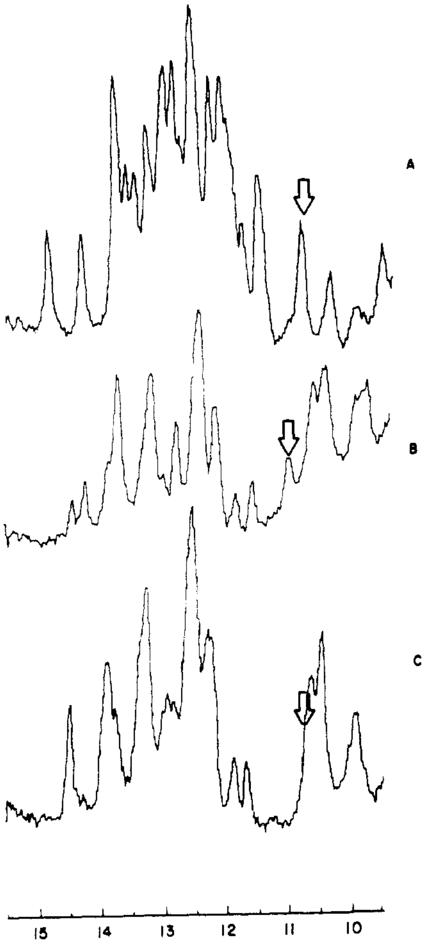

FIGURE 1: Imino proton spectra. (A) Sample 1, *E. coli* tRNA^{Val} dialyzed vs. 100 mM NaCl, 10 mM phosphate, pH 7, 1 mM EDTA, and 1 mM $Na_2S_2O_3$. (B) Sample 4, yeast tRNA^{Phe} dissolved in 100 mM NaCl, 10 mM cacodylate, pH 7, and 10 mM EDTA. (C) Sample 5, yeast tRNA^{Phe}, dialyzed vs. 100 mM NaCl, 10 mM phosphate, pH 7, and 5 mM $MgCl_2$. The horizontal scale is in parts per million from DSS; the arrows indicate the positions of Ψ_{55} N_1 proton, assignment of which is described under Results.

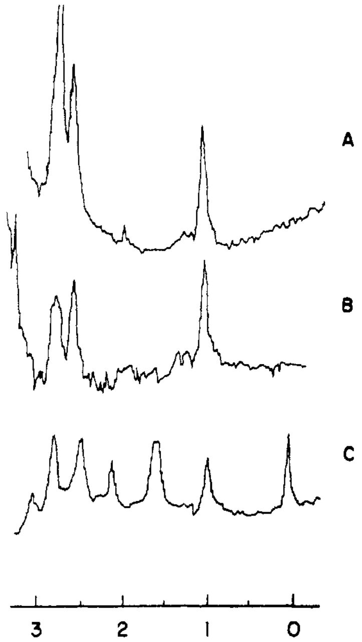

FIGURE 2: Methyl proton spectra. Solvent conditions were as described in Figure 1 and under Materials and Methods. (A) *E. coli* tRNA^{Val}, sample 1.1. The large peak near 2.8 ppm is due to EDTA. (B) *E. coli* tRNA^{Val}, sample 2. (C) Yeast tRNA^{Phe}, sample 5. The T methyl resonance is at ~1 ppm in all cases. The sharp peak at 0 ppm in (C) is of unknown origin.

a small shoulder at 7.28 ppm, as well as a medium-sized effect to the resolved exchangeable proton resonance at 10.78 ppm (Figure 4A,B; Table II). Saturation of the 10.78 ppm resonance gives a large effect at 7.28 ppm with a small shoulder at 7.42 ppm, as well as a medium-sized effect to the T methyl (Figure 6, Table II). We believe that both effects observed at 7.42 ppm arise from a single proton; likewise the two effects at 7.28 ppm represent a single proton.

The T_{54} Methyl Resonance Is Well Established To Be at 0.96 ppm. All thymine-containing tRNAs studied to date show a resonance of intensity of three protons at ~1 ppm downfield of DSS. This resonance was first assigned to the T methyl in yeast tRNA^{Phe} by Kan et al. (1974, 1977) and also confirmed by Robillard et al. (1977). The assignment in *E. coli* tRNA^{Val} was made by Kastrup & Schmidt (1975, 1978); the assignment in *E. coli* tRNA^{fmet} was made by Davanloo et al. (1979). The yeast initiator tRNA, which lacks thymine, does not show a resonance near 1.0 ppm (Figueroa and A. G. Redfield, unpublished experiments).

The NOE's at 7.42 ppm Are Assigned to the C_6 Proton of

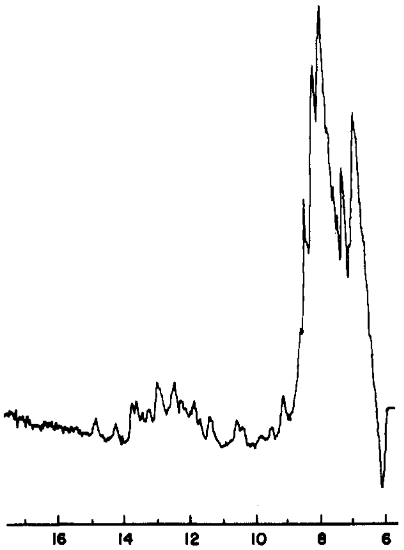

FIGURE 3: *E. coli* tRNA$^{\text{Val}}$, sample 3. Solvent conditions were as described under Materials and Methods. The horizontal scale is in parts per million from DSS.

Residue T_{54}. The 7.42-ppm effect is the largest effect observed *from* the T methyl (Figure 4A), and its reciprocal NOE is the largest effect observed *to* the T methyl. This is consistent with the expectation that C_6-H should be the closest proton neighbor of the T methyl group. Furthermore, the measured σ value yields the distance to the methyl group (3.1 Å, Table II) to within 0.2 Å of the value calculated from thymine atomic coordinates (Table I). The small effect from 10.78 to 7.42 ppm (Figure 6A) is consistent with the assignment of the 10.78-ppm resonance to the N_1 proton of residue Ψ_{55}, as discussed below.

The NOE at 10.78 ppm Is Assigned to the N_1 Proton of Residue Ψ_{55}. First, this proton is predicted to be non hydrogen bonded in the tRNA$^{\text{Phe}}$ crystal structure, and imino protons of the free nucleoside Ψ give a broad resonance between 10 and 11 ppm in aqueous solution near neutral pH (P. Johnston, unpublished experiments). Second, barring gross structural differences between the tRNA$^{\text{Phe}}$ crystal structure and the tRNA$^{\text{Val}}$ solution structure, the Ψ N_1-H proton is the only imino (or amino) proton within 4 Å of the T methyl group and is therefore the only likely candidate for an exchangeable proton NOE from the T methyl. The distance between the N_1 proton and the methyl group is calculated from the σ value to be 3.9 Å (r_c, Table II), in good agreement with the range of values (3.4–4.1 Å) calculated from the tRNA$^{\text{Phe}}$ crystal coordinates (Table I). Third, the Ψ C_6 proton, which should resonate in the aromatic amino region, is 2.3 Å distant from the Ψ N_1 proton, so that irradiation at 10.78 ppm should produce a large NOE in the region 6–8 ppm. Such an effect is in fact observed (Figure 6A, Table II) at 7.28 ppm. Note that such an NOE would *not* be expected between the N_3 and C_6 protons of Ψ_{55}, which are roughly 4.5 Å apart. Furthermore, the fact that an NOE occurs at 7.28 ppm rather than at 7.42 ppm excludes the possibility that the effect from the T methyl to 10.78 ppm is a second-order effect transmitted through the T C_6 proton. Fourth, since the 10.78-ppm resonance gives a medium-sized NOE (11%) to the T methyl, which in turn gives a large (50%) effect to the T C_6-H, irradiation at 10.78 ppm should produce a small second-order effect (10% × 50% = 5%) at 7.42 ppm. Alternatively, the theoretical σ between the Ψ N_1 and T C_6 protons is 0.4/s, which could give a first-order effect of a few percent. A combination of first- and second-order effects could also occur. In fact, a small but distinct shoulder at exactly 7.42 ppm is observed upon saturation at 10.78 ppm (Figure 6A; see also Figure 6B), in agreement with these predictions.

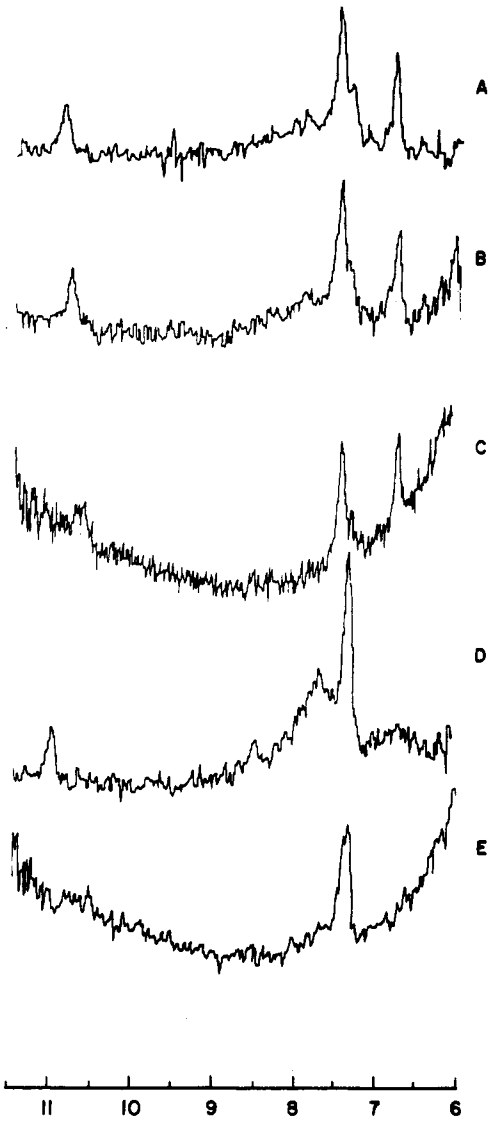

FIGURE 4: NOE difference spectra arising from saturation of T methyl resonance. Spectra were obtained as described under Materials and Methods by using a 200-ms satuation pulse. The horizontal scale is in parts per million from DSS. (A, B, and C) *E. coli* tRNA$^{\text{Val}}$, samples 1, 2, and 3, respectively. (D and E) Yeast tRNA$^{\text{Phe}}$, samples 4 and 5.

The NOE's at 7.28 ppm Are Assigned to the C_6 Proton of Residue Ψ_{55}. The assignment of the large NOE at 7.28 ppm from 10.78 ppm has been discussed above. It remains to discuss the small shoulder at 7.28 ppm which arises from saturation of the T methyl resonance (Figure 4A). As in the case of the small effect at 7.42 ppm, the small effect at 7.28 ppm could be second order (transmitted from the T methyl via the N_1 proton) or first order, or a combination of the two. Since σ in this case is quite small (0.1/s), we believe that a pure first-order effect is unlikely.

The NOE at 6.73 ppm Is Tentatively Assigned to the C_8 Proton of Residue G_{53}. This NOE lies on the border between the aromatic amino and ribose backbone regions of the spectra. Similar NOE's are found at 6.73 ppm in *E. coli* tRNA$^{\text{fMet}}$ (see below) and at 6.76 ppm in yeast tRNA$^{\text{Ala}}$ (V. Sânchez, unpublished experiments), but not in yeast tRNA$^{\text{Phe}}$ (Figure 4D,E). The striking closeness of the NOE's in tRNA$^{\text{Val}}$, tRNA$^{\text{fMet}}$, and tRNA$^{\text{Ala}}$ may be correlated with the common T arm sequence GGTΨC; the corresponding sequence in tRNA$^{\text{Phe}}$ is UGTΨC.

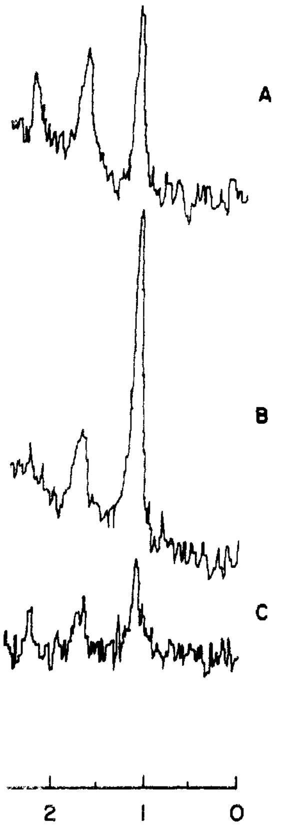

FIGURE 5: Action spectrum from aromatic amino region to T methyl resonance (1 ppm) for sample 5, yeast tRNA^{Phe}. (A) Saturation at 7.14 ppm, 0.2 ppm upfield of T C_6 proton. (B) Saturation at 7.34 ppm, directly on the resonance for the T C_6 proton. (C) Saturation at 7.54 ppm, 0.2 ppm downfield of T C_6 proton. The saturation pulse was 200 ms in all cases.

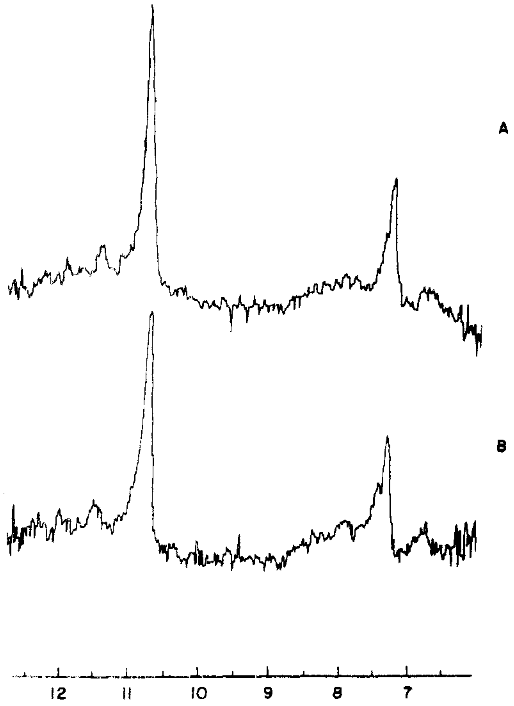

FIGURE 6: NOE spectra from putative Ψ_{55} N_1 proton to aromatic amino region. The large peak at 10.78 ppm is from direct irradiation; The NOE's appear at ~7.3 ppm. (A) Sample 1, *E. coli* tRNA^{Val}; (B) sample 2, *E. coli* tRNA^{Val}.

The NOE in yeast tRNA^{Ala} is missing from samples which are biosynthetically deuterated at all purine C_8 positions (V. Sânchez, unpublished experiments); therefore it represents a C_8 proton. According to the yeast tRNA^{Phe} crystal structure, the only C_8 proton close enough to experience an NOE from the T methyl is that of residue G_{53}. The cross relaxation rate calculated from tRNA^{Phe} atomic coordinates is 0.5 s^{-1}, which is close to the experimental value obtained for tRNA^{Val} (Table II). We note that 6.73 ppm is an unusual position for a purine C_8 proton resonance.

Table III: Summary of NOE Data and Internuclear Distances Inferred from Them for Yeast Phenylalanine tRNA[a]

irradiated resonance	obsd resonance: 0.98 ppm (0.96),[b] T_{54} methyl	7.34 ppm, T_{54} C_6-H and Ψ_{55} C_6-H	10.96 ppm (10.65), Ψ_{55} N_1-H
0.98 ppm (0.96), T_{54} methyl		>50%	5% (0%)
7.32 ppm, T_{54} C_6-H and Ψ_{55} C_6-H	50% $\sigma = 2.8/s$ $r_c = 3.0$ Å[c]		not obsd[d]
10.96 ppm (10.65), Ψ_{55} N_1-H	9% $\sigma = -0.5$ $r_c = 4.1$ Å	>50%	

[a] Notation and conditions are as described for Table II. Data are for sample 4 (0 Mg) except where a significant difference is observed in the presence of Mg (sample 5), in which case sample 5 data are given in parentheses. [b] The longitudinal relaxation rate ρ for the T methyl was 4.5 s^{-1}. [c] The r_c value is given for the T_{54} C_6 protons. The value of σ in this case agrees exactly with that calculated from thymine coordinates, but the tabulated r_c is derived from the approximate model geometry described earlier in the text. [d] Possible NOE obscured by nonspecific effect.

(*B*) *Sample 3, E. coli tRNA^{Val}*. A typical NOE appears in Figure 4C. The NOE data were recorded with low saturation power and are therefore not sufficiently accurate to justify internuclear distance calculations, but the presence of Mg^{2+} ion does not cause any gross alteration in the pattern of NOE's. The only change upon addition of Mg^{2+} is the upfield shift of the resonance assigned to the Ψ_{55} N-H proton from 10.78 ppm in 0 Mg^{2+} to 10.57 ppm. All other NOE's lie within 0.02 ppm of the corresponding effects in the Mg^{2+} free samples.

(*C*) *Sample 4, Yeast tRNA^{Phe} in 0 Mg^{2+}*. Figure 4D shows the NOE spectrum obtained upon saturation of the T methyl resonance. The pattern is somewhat similar to those obtained for *E. coli* tRNA^{Val}, with a large effect at 7.34 ppm and a medium effect at at 10.96 ppm. However, the 7.34-ppm effect does not show any small resolved shoulder, and saturation of the 10.96-ppm resonance gives a large NOE to exactly 7.34 ppm.

The broad effect at 7.7 ppm is apparently due to power spillover from saturation of the T methyl. Lowering the saturation power causes this peak to disappear, while other NOE's are only slightly attenuated.

The NOE's Observed at 7.34 ppm Arise from Two Coincidentally Overlapping Resonances: the C_6 Protons of Residues T_{54} and Ψ_{55}. It is reasonable that these two protons, which resonate at 7.28 and 7.42 ppm in *E. coli* tRNA^{Val}, could coincide at 7.34 ppm in yeast tRNA^{Phe}. The magnitudes of the NOE's (Table III) are consistent with this conclusion. Independent evidence comes from consideration of the second-order NOE that would be observed if the NOE's at 7.34 were in fact due to a single proton. We find a 50% NOE from 10.96 to 7.34 ppm and a 50% NOE from 7.34 ppm to the T methyl. Thus we would predict a second-order NOE of 0.5 × 0.5 or 25%, from 10.96 ppm to the T methyl. In fact, the observed NOE is only 9%, in good agreement with similar effects in tRNA^{Val}, which are clearly first order.

Table IV: Summary of NOE Data and Internuclear Distances Inferred from Them for *E. coli* Formylmethionine tRNA[a]

	obsd resonance				
irradiated resonance	0.96 ppm, T_{54} methyl[b]	6.76 ppm, G_{53} C_8 (?)	7.27 ppm, Ψ_{55} C_6-H	7.44 ppm, T_{54} C_6-H	10.61 ppm, Ψ_{55} N_1-H
0.96 ppm, T_{54} methyl		14%	not obsd[c]	>40%	10%
6.76 ppm, G_{53} C_8	19% $\sigma = 1.6$/s $r_c = 3.5$ Å				
7.44 ppm, T_{54} C_6-H	33% $\sigma = 2.7$/s $r_c = 3.1$ Å	not obsd[c]	not obsd[c]		not obsd[c]
10.61 ppm, Ψ_{55} N_1-H	16% $\sigma = 0.9$/s $r_c = 3.8$ Å	0%	40%	<3%	

[a] Notation is as described for Tables II and III. [b] The longitudinal relaxation rate for the T methyl group was 5.4/s. [c] Possible NOE obscured by power spillover or nonspecific effects.

T_{54} and Ψ_{55} Assignments and Structure Are Virtually Identical with Those Found Above for tRNA^{Val}. Once the point just discussed is established, the assignments proceed in an obvious way, and interproton distance estimates are in good agreement with those of Tables I and II.

A Small NOE at 8.4 ppm Is Tentatively Assigned to the C_8 Proton of Residue G_{53}. Despite its small size (roughly 5%) this NOE is reproducibly observed in all Mg^{2+}-free samples we have studied (Figure 4C), with the following exception. In tRNA^{Phe} which is biosynthetically deuterated at all purine C_8 positions (Sânchez et al., 1980), the NOE is missing. The C_8 proton of residue G_{53} is the most likely candidate for this NOE.

This NOE is not observed in samples containing Mg^{2+}, possibly because of a small conformation change, whereas the 6.73 ppm NOE assigned to the G_{53} C_8 proton in tRNA^{Val} is not sensitive to Mg^{2+}. Also, it is hard to rationalize the large chemical shift difference between the proposed G_{53} C_8 resonances in tRNA^{Phe} and tRNA^{Val}.

(D) Sample 5, Yeast tRNA^{Phe} in 5 mM Mg^{2+}. The NOE spectrum resulting from saturation of the T methyl resonance in sample 5 (Figure 4E) shows a large effect at 7.34 ppm, as in sample 4, but no effect is observed in the region 10–11 ppm. However, irradiation at 10.65 ppm produces a 50% NOE at exactly 7.34 ppm and a 10% effect at the T methyl. An action spectrum through the composite peak spanning 10.5–10.7 ppm (Figure 1) shows that these effects are specific and that their maxima occur at the same frequency, so that they almost certainly arise from saturation of the same buried proton. Thus, the pattern of NOE's between residues T_{54} and Ψ_{55} is in essence the same for this sample as for those discussed above, with the Ψ_{55} N_1 proton resonating at 10.65 ppm in the present case. The failure to observe an NOE *to* 10.65 ppm is probably due to an increased rate of solvent exchange for the Ψ_{55} N_1-H in the presence of Mg^{2+}. Data for tRNA *E. coli* tRNA^{Val} (J. Tropp, A. G. Redfield, and V. Sânchez, unpublished experiments) show that addition of Mg^{2+} *increases* the exchange rate of this proton, and we expect that the same holds true for yeast tRNA^{Phe}.

The upfield shift (from 10.96 to 10.65 ppm) observed upon addition of Mg^{2+} is to be expected on the basis of both the results given above for *E. coli* tRNA^{Val} and those from a $MgCl_2$ titration of yeast tRNA^{Phe} reported elsewhere (Johnston & Redfield, 1981).

(E) Sample 6, E. coli tRNA^{fMet} in 0 Mg^{2+}. The NOE data and calculated distances are given in Table IV; the NOE spectra are not shown. Apart from small differences in resonance positions, the pattern of NOE's is virtually identical with that observed in tRNA^{Val}; accordingly, all assignments are made by analogy. The Ψ_{55} N_1 proton is well resolved in the absence of Mg^{2+}.

Discussion

Resonance Assignments. The assignment of low-field proton resonances in tRNA has proven difficult. It is now acknowledged that assignments based on ring-current calculations are suggestive at best (Bolton & Kearns, 1978) and must be confirmed by independent methods such as specific chemical modifications or NOE studies (Schimmel & Redfield, 1980). A resonance assignment is useful only inasmuch as it is known to be correct; therefore *every* proposed assignment should be critically assessed. We regard our present assignments of Ψ_{55} N_1 protons as highly reliable but not incontrovertible.

The assignments were reached by a process of elimination: It is difficult to explain the presence of an exchangeable proton within a radius of 4 Å of the T methyl group by *any* hypothesis other than that which we have given. The T methyl assignment itself seems reliable. The experimentally determined distance between the Ψ N_1 proton and the center of the T methyl group derives from a cross relaxation calculation involving an assumed molecular geometry, but virtually *any* other geometry would lead to a distance between 3.5 and 4.0 Å (Tropp, 1980). The calculation contains no adjustable parameters and is relatively insensitive to the value of the rotational diffusion constant, as noted earlier. Finally, the large NOE from the putative Ψ_{55} N_1-H resonance to the aromatic regions excludes the possibility that we are observing the N_3 proton of Ψ_{55}. The excellent agreement for the σ values observed from the T_{54} C_6 resonance to the T_{54} methyl resonance (2.3–2.8 s^{-1}) compared to theory (2.8 s^{-1}) is an indicator that the distance estimates and general approach are realistic.

Structural Implications. The present study demonstrates the base stacking of residues Ψ_{55} and T_{54} in the solution structures of three class I tRNAs. The relative magnitudes of the NOE's from the T methyl to the N_1 and C_6 protons of Ψ_{55} suggest that the details of stacking geometry are similar in solution and in the crystal; the crystal geometry is illustrated in Figure 7. The conclusion that it is in fact the N_1 proton rather than the N_3 proton of Ψ_{55} which lies over the methyl group confirms that the glycosidic conformation of Ψ_{55} is correctly assigned in the crystal structure.

The observation that the cross relaxation rates between the Ψ_{55} N_1 and T methyl protons are unaffected by Mg^{2+} indicates that the stacking distance between residues 54 and 55 is unchanged. However, the upfield shift of the N_1-H resonance when Mg^{2+} is added and the loss of the NOE from the T

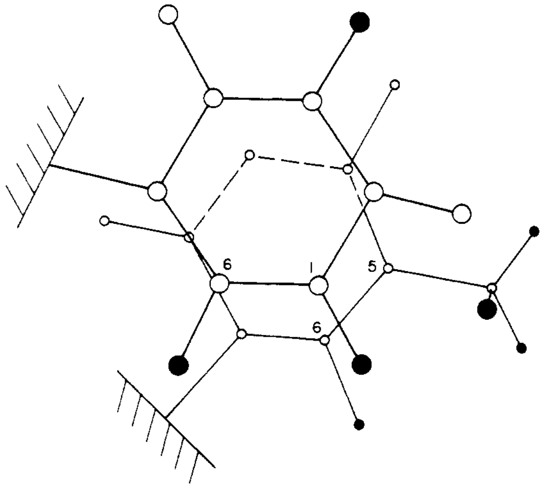

FIGURE 7: Stacking geometry of residues T_{54} (below) and Ψ_{55} (above), according to the crystal structure of yeast tRNA^{Phe}. The ring and methyl protons are shown in solid black for emphasis; all other atoms are shown as open circles.

methyl to the N_1 proton in tRNA^{Phe} both suggest some sort of structural event induced by Mg^{2+}. Our naive expectation is that a large resonance shift (0.2 ppm) for the N_1 proton should be accompanied by similar shifts in the adjacent NOE-coupled protons, but the neighbor proton shifts are all <0.02 ppm. A possible explanation is that binding of Mg^{2+} causes expulsion of a water molecule which was hydrogen bonded to the N_1 proton. This could account for the large upfield shift and the small perturbation of other resonances. In any case, arguments based on the premise that binding of a small molecule should produce shifts of comparable magnitude for all protons in the vicinity of binding should be treated with caution.

Acknowledgments

We thank Valentina Sânchez for expert assistance in purifying tRNA and for communicating her results on C_8 deuterated yeast tRNA^{Ala}.

References

Bolton, P., & Kearns, D. (1978) in *Biological Magnetic Resonance* (Berliner, L. J., & Reuben, J., Eds.) p 91, Plenum Press, New York.

Bothner-By, A. A. (1979) in *Biological Applications of Magnetic Resonance* (Shulman, R. G., Ed.) p 177, Academic Press, New York.

Davanloo, P., Sprinzl, M., Watanabe, K., Albani, M., & Kersten, H. (1979) *Nucleic Acids Res. 6*, 1571.

Dubs, A., Wagner, G., & Wüthrich, K. (1979) *Biochim. Biophys. Acta 577*, 177.

Johnston, P. D., & Redfield, A. G. (1977) *Nucleic Acids Res. 4*, 3599.

Johnston, P. D., & Redfield, A. G. (1978) *Nucleic Acids Res. 5*, 3913.

Johnston, P. D., & Redfield, A. G. (1979) in *Transfer RNA: Structure, Properties, and Recognition* (Abelson, J., Schimmel, P., and Söll, D., Eds.) p 191, Cold Spring Harbor Press, Cold Spring Harbor, NY.

Johnson, P. D., & Redfield, A. G. (1981) *Biochemistry 20*, 1147.

Kalk, A., & Berendsen, J. C. (1976) *J. Magn. Reson. 24*, 343.

Kan, L. S., Ts'o, P. O. P., von der Haar, F., Sprinzl, M., & Cramer, F. (1974) *Biochem. Biophys. Res. Commun. 59*, 22.

Kan, L. S., Ts'o, P. O. P., von der Haar, F., & Cramer, F. (1977) *Biochemistry 16*, 3143.

Kastrup, R. V., & Schmidt, P. G. (1975) *Biochemistry 14*, 3612.

Kastrup, R. V., & Schmidt, P. G. (1978) *Nucleic Acids Res. 5*, 257.

Kim, S. H., Suddath, F., Quigley, G., McPherson, A., Sussman, J., Wang, A., Seeman, N., & Rich, A. (1974) *Science (Washington, D.C.) 185*, 435.

Komoroski, R. A., & Allerhand, A. A. (1972) *Proc. Natl. Acad. Sci. U.S.A. 69*, 1804.

Ladner, J. E., Jack, A., Robertus, J. D., Brown, R. S., Rhodes, D., Clark, B. F. C., & Klug, A. (1975) *Nucleic Acids Res. 2*, 1629.

Noggle, J. H., & Schirmer, R. E. (1971) *The Nuclear Overhauser Effect*, Academic Press, New York.

Redfield, A. G. (1976) *NMR: Basic Princ. Prog. 13*, 137.

Redfield, A. G., & Gupta, R. K. (1971) *Cold Spring Harbor Symp. Quant. Biol. 36*, 405.

Redfield, A. G., & Kunz, S. (1979) in *NMR and Biochemistry* (Opella, S., & Lu, P., Eds.) p 225, Marcel Dekker, New York.

Robillard, G. T., Tarr, C. E., Vosman, F., & Reid, B. R. (1977) *Biochemistry 16*, 5261.

Sânchez, V., Redfield, A. G., Johnston, P., & Tropp, J. (1980) *Proc. Natl. Acad. Sci. U.S.A. 77*, 5659.

Schimmel, P., & Redfield, A. G. (1980) *Annu. Rev. Biophys. Bioeng. 9*, 181.

Schmidt, P. G., Tompson, J., & Agris, P. F. (1980) *Nucleic Acids Res. 8*, 644.

Sigler, P. B. (1975) *Annu. Rev. Biophys. Bioeng. 4*, 477.

Stoesz, J. D., Malinowski, D. P., & Redfield, A. G. (1979) *Biochemistry 18*, 4669.

Stout, D. C., Mizuno, H., Rubin, J., Brennan, T., Rao, S. T., & Sundaralingam, M. (1976) *Nucleic Acids Res. 3, 1111.*

Sussman, J. L., Holbrook, S. R., Warrant, R. W., Church, G. M., & Kim, S. H. (1978) *J. Mol. Biol. 123*, 607.

Tao, T., Nelson, J. H., & Cantor, C. R. (1970) *Biochemistry 9*, 3514.

Tropp, J. (1980) *J. Chem. Phys. 72*, 6035.

Voet, D., & Rich, A. (1970) *Prog. Nucleic Acid Res. Mol. Biol. 10*, 183.